Uranyl Ion Extraction with Conventional PUREX/TRUEX Ligands Assessed by Electroanalytical Chemistry at Micro Liquid/Liquid Interfaces

ARTICLE *in* ANALYTICAL CHEMISTRY · AUGUST 2011

Impact Factor: 5.64 · DOI: 10.1021/ac2018684 · Source: PubMed

2 AUTHORS:

T. Jane Stockmann
Paris Diderot University
20 PUBLICATIONS **124** CITATIONS
SEE PROFILE

Zhifeng Ding
The University of Western Ontario
123 PUBLICATIONS **3,280** CITATIONS
SEE PROFILE

analytical chemistry

ARTICLE

pubs.acs.org/ac

Uranyl Ion Extraction with Conventional PUREX/TRUEX Ligands Assessed by Electroanalytical Chemistry at Micro Liquid/Liquid Interfaces

Tom J. Stockmann and Zhifeng Ding*

Department of Chemistry, The University of Western Ontario, Chemistry Building, 1151 Richmond Street, London, Ontario, Canada N6A 5B7

ABSTRACT: The facilitated ion transfer (FIT) of uranyl or dioxouranium (UO_2^{2+}) was studied electrochemically using a micro interface between two immiscible electrolytic solutions (micro-ITIES) in order to evaluate the complexation stoichiometry and complexation constants (β) of two widely used ligands in spent fuel reprocessing: tributylphosphate (TBP) and octyl(phenyl)-*N*,*N*-diisobutylcarbamoylmethyl-phosphine oxide (CMPO). For the first time, discrete interfacial complexation reaction steps of varying uranyl to the two ligands ratios were resolved using the micro-ITIES hosted at the tip of a 25 μm diameter glass capillary. Two stoichiometries for $UO_2NO_3TBP_n^+$ were determined including n = 3 and 4 with β values of 3.2×10^{11} and 3.9×10^{13}, respectively. Subsequently, three distinct complexation reactions of CMPO with UO_2^{2+} were discovered corresponding to $UO_2NO_3CMPO_2^+$, $UO_2NO_3CMPO_3^+$, and $UO_2CMPO_5^{2+}$ whose respective complexation constants were determined to be 8.0×10^{11}, 8.8×10^{14}, and 6.5×10^{32}. The participation of nitrate anions in these complexation reactions is also discussed.

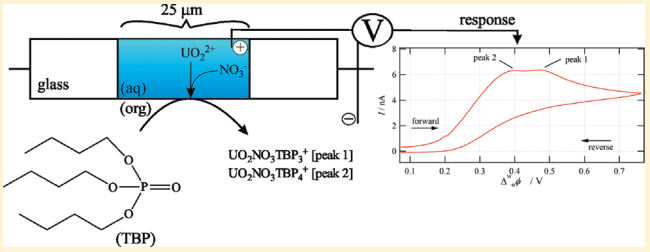

The continued debate over climate change has sparked a resurgence of interest in alternative energy resources to replace fossil fuels, included in these is nuclear power generation. One of the most effective nuclear power generation techniques has been the Canadian Deuterium Uranium (CANDU) heavy water reactors, owing to their capability to utilize natural sources of uranium and even spent nuclear fuel from conventional light water reactors.[1−4] This ability stems from the high efficiency of neutron capture within the deuterium heavy water system and the use of materials, such as zirconium, which have a minimal neutron absorption cross-section.[5] Fission products, however, have high neutron absorptions and limit the lifetime of the fuel bundle despite the continued presence of significant fissile material.[4] Additionally, it has been demonstrated that recycled uranium fuel, with 0.9% ^{235}U, shows improved energy production versus naturally occurring uranium[4] in a CANDU reactor. Therefore, of particular interest is the recycling/reprocessing of nuclear fuels to remove high neutron absorbers and reclaim valuable energy producing nuclear isotopes, extending the life of nuclear fuel.

Additionally, since the unfortunate events of March 11, 2011 which saw a massive earthquake generated tsunami cripple the Japanese Fukushima nuclear power plant, techniques toward nuclear waste cleanup or environmental reclamation of nuclear waste contaminated regions are also of practical interest. The Plutonium URanium EXtraction (PUREX) process has been the dominant method of nuclear fuel reprocessing for half a century,[6−8] with an improvement to the process being introduced toward the end of the 1980s in the form of the TRans-URanium EXtraction (TRUEX) process.[6,9−14] Both methods are solvent extraction techniques using an aqueous|organic interface and phosphine oxide organic ligands.[6−14] The PUREX process utilizes tributylphosphate (TBP)[6−8,10,15] as the primary ligand, while TRUEX uses a combination of TBP and octyl(phenyl)-*N*,*N*-diisobutylcarbamoylmethyl-phosphine oxide (CMPO).[6,9,13,16−21] Since its inception, the TRUEX process has employed TBP to gain improved selectivity and specificity for transuranic elements[16,18] and prevent the formation of a third emulsion phase. Conventional uranium reprocessing, using *n*-dodecane as the solvent, makes use of a series of centrifugal reactors whose engineering complexity is intimidating but necessary in order to achieve the degree of selectivity and recovery. Maintenance costs for this equipment is high, owing to its saturation with radioactive material, and this process also generates a considerable quantity of radioactive raffinate. Thus, a simplified cost-effective technique toward the separation of these valuable materials is desirable. Recently, the focus of research has switched from the development of new ligands to alternative solvents such as room temperature ionic liquids (organic salts whose melting point is less than 100 °C)[10−12,15,22−27] which have demonstrated high distribution ratios in metal extraction.[10,11,14,22,26,27]

Predominant methods of analyzing the effectiveness of the TRUEX extraction process, conducted with these alternative solvents, has utilized radioactive tracer elements in order to monitor metal distribution ratios between the two phases[19,20] or expensive analytical techniques such as inductively coupled

Received: July 20, 2011
Accepted: August 17, 2011
Published: August 17, 2011

plasma.[22] This analysis is often carried out in the presence of both CMPO and TBP, specifically a solution of 0.2 M CMPO and 1.2 M TBP,[9,19,20,28,29] on the industrial scale. However, the continued role of CMPO and TBP in these alternative solvents is still of interest and yet to be identified. Therefore, in the current study, they were evaluated individually through an inexpensive, facile electrochemical technique at a micro interface between two immiscible electrolytic solutions (micro-ITIES). In this initial study, a molecular organic solvent was used with the goal that the thermodynamic data obtained will be used for future comparison research toward RTIL electrochemical extraction methodologies. It should be noted that the common chemical form of uranium found in conventional PUREX or TRUEX processes is uranyl or dioxouranium,[6,7] UO_2^{2+}, with uranium in the 6+ oxidation state; this is owing to the dissolution of solid uranium using a 3−6 M nitric acid solution. Therefore the salt, $UO_2(NO_3)_2 \cdot 6H_2O$, was used in all analysis.

The ITIES, commonly between water and nitrobenzene (NB)[30,31] (w|NB) or 1,2-dichloroethane (DCE)[30,32−38] (w|DCE), has been developed as a powerful technique for the evaluation of ion transfer(IT)[37−42] and assisted or facilitated ion transfer (FIT)[31,33−36,43−46] using cyclic voltammetry (CV). The simple IT mechanism can be shown through the following relationship:

$$i^{z_i}(w) \rightleftharpoons i^{z_i}(o) \quad (1)$$

where species i, with charge z_i, transfers from the aqueous phase (w) to the organic phase (o). Complexation of a metal ion, interfacially with ligands in the organic phase lowers the metals Gibb's free energy of transfer, increasing its miscibility toward the organic phase and results in increased partitioning of the ion from $w \rightarrow o$; this describes the principle of FIT and is shown in eq 2,

$$M^{z+}(w) + nL(o) \rightleftharpoons ML_n{}^{z+}(o) \quad (2)$$

where the metal species, M, coordinates to n ligand molecules, L. The theory of electroanalytical chemistry at an ITIES has been developed for both IT[37,38,47] and FIT.[36,44,45] A convenient method of generating and maintaining an ITIES of known dimensions is by micro-ITIES.[32,37,38,48,49] The interface can be prepared by submerging a pulled borosilicate glass capillary, with an aqueous phase inside, into a vial containing the organic/DCE phase; the interface is held at the tip of the micropipet. Micro-ITIES is advantageous since the low current required to perform a CV experiment results in a negligible iR-drop[37] and can employ a simple two-electrode system. The microscale of the experiment results in rapid ion transfer generating sensitive kinetic measurements[38] and, in conjunction with the asymmetric diffusion regime, linear diffusion inside the pipet and hemispherical outside allows for the discrimination of species based on their charge. The methodology for FIT has been developed, and experimental data have been accumulated utilizing a large-ITIES[44,45] which can be used to describe the stoichiometry, the metal to ligand ratio (1:n), and the overall complexation constant, β, of the reaction shown in eq 2. These can be extrapolated to the micro-ITIES,[36] harnessing its sensitivity. The two apparent thermodynamic parameters were quantified with respect to the traditional PUREX and TRUEX ligands, TBP[6,7,10,15] and CMPO.[6,9,13,16−20] However, to the best of our knowledge, it is for the first time at a micro-ITIES, that complexes of varying coordination numbers are resolved simultaneously. This level of resolution, combined with the microscale, will be of interest to those developing ion-selective electrodes, as recently demonstrated by Samec et al.,[43] for the identification of metal species in solution.

EXPERIMENTAL SECTION

Chemicals. All chemicals were of reagent grade and used as purchased without further purification. Tri-*n*-butylphosphate (TBP), tetradodecylammonium tetrakis(4-chlorophenyl)borate (TDATPBCl), 1,2-dichloroethane (DCE) (anhydrous), lithium sulfate monohydrate ($Li_2SO_4 \cdot H_2O$), and tetrabutylammonium perchlorate ($TBAClO_4$) were obtained from Fluka/Sigma-Aldrich (Fluka/Sigma-Aldrich Canada limited, Mississauga, ON). Octyl(phenyl)-*N*,*N*′-diisobutylcarbamoylmethylphosphine oxide (CMPO) was bought from Strem Chemicals (Strem Chemicals Inc., Newburyport, MA). Uranyl nitrate hexahydrate was purchased from Fisher Scientific (Thermo Fisher Scientific Canada, Ottawa, ON); all aqueous solutions were prepared using 18.2 MΩ Milli-Q water.

Micro-ITIES. The micro-ITIES experimental setup consisted of a specialized micro-ITIES glass capillary, containing a silver electrode (the working electrode) and the aqueous phase, that was held in a Heka capillary holder (HEKA Electronics, Mahone Bay, NS), and a 4 mL glass vial which contained the organic phase and a second silver electrode. A very stable micro-ITIES can be established in this way.

The specialized micro-ITIES capillary was fabricated by first pulling a borosilicate glass capillary (1.0/2.0 inner diameter/outer diameter) using an electric-heating coil puller (Narishige, Model# PP-83, Japan) generating two tapered capillaries. Pt wire was then heating-annealed at the tapered end using the puller, which was subsequently polished using diamond grinding pads and aluminum oxide, Fibrmet discs (Buehler Canada, Markham, ON), to expose a cross-section of the Pt wire and smooth the glass surface. The glass capillary was polished to yield a ratio of the outer glass radius (r_g) to an inner, metal wire radius (a), of >50 (defined as the R_g ($R_g = r_g/a$)). The Pt wire was subsequently removed using a strong acid etching solution of 3:1 HCl/HNO_3 to expose a microhole 25 μm in diameter. A detailed description of this process can be found elsewhere.[32]

The pipet holder was equipped with a syringe which, under pressure, sustained the aqueous phase and subsequently the liquid−liquid interface at the tip of the glass capillary. The glass capillary was then submerged into the organic (DCE) phase contained in the small glass vial; careful attention was paid to maintaining the aqueous−organic interface at the orifice of the micropipet by means of the attached syringe under monitoring of an optical microscope. A second silver electrode, which served as both the counter and reference electrodes, was then placed in the organic phase. The electrochemical cells for the micro-ITIES are detailed below:

Ag	$AgNO_3$	5 mM $UO_2(NO_3)_2 \cdot 6H_2O$ (aq)	5 mM TDATPBCl, y mM TBP (DCE)	AgTPBCl	Ag	Cell 1
Ag	$AgNO_3$	5 mM $UO_2(NO_3)_2 \cdot 6H_2O$ (aq)	5 mM TDATPBCl, y mM CMPO (DCE)	AgTPBCl	Ag	Cell 2
Ag	$AgNO_3$	0.5 mM $UO_2(NO_3)_2 \cdot 6H_2O$ (aq)	5 mM TDATPBCl (DCE)	AgTPBCl	Ag	Cell 3

Instrumentation. Electrochemical measurements were performed using the Modulab System from Solartron Analytical (Ametek Advanced Measurement Technology, Farnborough, Hampshire, United Kingdom) equipped with a Femto ammeter and using a feedback control loop.

Calibration of the Polarizable Potential Window (PPW). Simple IT of the nitrate anion (NO_3^-) was used to calibrate the polarizable potential window (PPW) according to the TATB assumption,[50−52] whereby the formal transfer potential of NO_3, $\Delta_o^w\phi_{NO_3^-}^{o'}$, was taken to be −0.314 V.[30] By convention, the transfer of a positively charged species from aqueous to organic generates a positive peak current and the transfer of a negatively charged species generates a negative peak current. The TATB assumption results in eq 3.[52]

$$\Delta_o^w\phi_{1/2,ML_n^{z+}} - \Delta_o^w\phi_{1/2,NO_3^-} = \Delta_o^w\phi_{ML_n^{z+}}^{o'} - \Delta_o^w\phi_{NO_3^-}^{o'} \quad (3)$$

The half wave potential ($\Delta_o^w\phi_{1/2}$) of nitrate and the metal complex were obtained by evaluating the limiting current (i_l) of the steady state wave and graphing $\Delta_o^w\phi$ vs $\log((i_l - i)/i)$, as detailed by Bard and Faulkner.[53] $\Delta_o^w\phi_{ML_n^{z+}}^{o'}$ is the formal transfer potential for the metal−ligand complex and $\Delta_o^w\phi_{M^{z+}}^{o'}$ is the formal transfer potential for the free metal species, UO_2^{2+}; free UO_2^{2+} IT was taken to be 0.865 V as reported elsewhere.[54]

NO_3^- was used as the internal reference since it is a common counterion in metal salts[6,22,55−57] and therefore already present. The nitrate concentration should remain relatively consistent throughout as it is housed in the aqueous phase inside the capillary and additions of the ligand were made directly to the DCE phase; this would cause a fluctuation in the concentration of any internal standard applied in that phase that would have to be addressed. Any changes in the concentration of the nitrate species could also be immediately recognized as fundamental to the extraction process and not an error in procedure. The formal transfer potential of the nitrate species is highly negative, directly opposed to any assisted metal transfer potentials, therefore, the nitrate transfer was unlikely to interfere with each other or overlap in the CV. Additionally, it is well recognized that NO_3^- participates in the assisted ion transfer of UO_2^{2+} during traditional PUREX and TRUEX industrial applications generating a neutral metal-nitrato species "$UO_2(NO_3)_2$".[6,55,56,58] While the participation of nitrate in the complexation reaction is well documented,[19] any replacement anion may have unknown or undesirable effects that may not be so easily recognized.

DCE was chosen as the molecular solvent since it has been widely studied in electrochemical solvent extraction systems.[33−36,41−46] Please note that all cyclic voltammograms (CVs) shown here have had their potential scale calibrated according to the NO_3^- IT.

RESULTS AND DISCUSSION

Facilitated Ion Transfer (FIT) of UO_2 Utilizing TBP. The first ligand to be examined was TBP, using Cell 1. Typical CVs while increasing the ligands concentration are shown in Figure 1.

During this series of CV experiments, the calibrated potential range was set from approximately −0.700 to 0.800 V; the range was altered in order to observe a wider potential window and ensure other peaks had not developed at higher (or lower) potentials. The first CV in Figure 1A is a "blank" one showing the system with no ligand present in the organic phase. The blank experiment begins by scanning in the forward direction, toward more positive potentials, with the initial potential equal to 0.000 V, which was determined by measuring the open circuit potential before each CV. The limit of the PPW is reached at 0.650 V; this limit is defined by the transfer of the supporting electrolytes, specifically tetrakis(4-chlorophenyl)borate anion (TPBCl) from

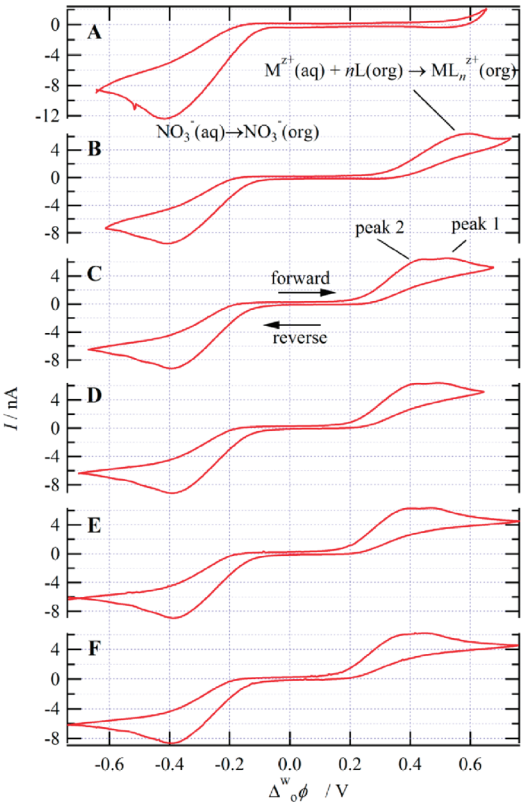

Figure 1. CVs obtained using Cell 1 and altering the concentrations of the ligand (y), TBP, in the organic phase to 0.0, 36.8, 64.3, 91.9, 110.2, and 128.2 mM for curves A, B, C, D, E, and F, respectively; the scan rate was set at 0.020 V·s^{-1}, with a calibrated potential range from −0.750 to 0.650 V and an initial potential of 0.0 V.

o→*w* and the free metal transfer of UO_2^{2+} from *w*→*o*. The scan direction was then reversed, heading toward more negative potentials. A peak shaped wave is observed at −0.400 V. This peak has been identified as the transfer of nitrate (NO_3^-), by linear diffusion, out of the aqueous phase, housed in the capillary, and into the organic phase (DCE), *w*→*o*. The half-wave potential for nitrate transfer can also be determined from the peak potential, using eq 4 below from Bard and Faulkner:[53]

$$\Delta_o^w\phi_{1/2} = \Delta_o^w\phi_p + 28.5/z_{eff}\,\text{mV} \quad (4)$$

In the case of nitrate transfer, the half-wave potential, $\Delta_o^w\phi_{1/2,NO_3^-}$, was determined to be −0.371 V. Subsequently, the lower limit of the PPW was reached at approximately −0.645 V, and this is defined by the Galvani transfer potential of the hydrophobic, organic supporting electrolyte tetradodecylammonium. The potential was then scanned again in the positive direction until the final potential of 0.000 V was reached. During this last segment, from −0.600 to 0.000 V, a sigmoidal wave was observed with a half wave potential at −0.314 V. This constitutes the hemispherical diffusion of NO_3^- toward the interface and transfer, across the ITIES, back into the aqueous phase; *o*→*w*. The asymmetric diffusion regime described is in agreement with established theory concerning IT at micropipet ITIES.[37,38] Considering the correction factor of 50 mV,[32] the two half-wave potential values determined above are in good agreement.

dx.doi.org/10.1021/ac2018684 |*Anal. Chem.* 2011, 83, 7542–7549

Figure 1B depicts the electrochemical behavior of the system with 36.8 mM of TBP in the DCE phase. During the initial forward scan, from 0.000 to 0.733 V, a positive peak shaped wave was observed at 0.588 V. This positive peak current was significant since it indicates the transfer of a positive ionic species. Subsequently, the potential was scanned from 0.733 to −0.614 V with a sigmoidal half-wave and negative peak-shaped wave potential obtained at 0.493 and −0.407 V, respectively. The sigmoidal wave is indicative of the hemispherical diffusion and transfer of a cation across the interface from $o \rightarrow w$, while the negative peak current indicates the continued presence of NO_3^- and its transfer from $w \rightarrow o$. The final portion of the voltammogram, scanned from −0.614 to 0.000 V, again shows the steady state current, i.e., hemispherical IT of the nitrate anion from $o \rightarrow w$.

Interestingly, with increasing concentrations of the ligand in the organic phase, the peak, originally observed at 0.588 V, shifts to more negative potentials. Figure 1C−F illustrates the system as the concentration of the ligand was increased further from 64.3 to 91.9, 110.2, and 128.2 mM with shifts in potential of 0.493, 0.458, 0.437, and 0.417 for curves C, D, E, and F, respectively. This shift in potential is indicative of FIT.[36,44,45] Since uranyl was the only free metal cationic species in the aqueous solution, according to Cell 1, and only the concentration of TBP was being altered, it was therefore concluded that the positive peak current obtained in Figure 1B−F is the result of assisted ion transfer of uranyl ions through a TIC mechanism with TBP acting as the ligand. With increasing ligand concentration, the half-wave potential of the hemispherical steady state curve decreases, analogous to the positive peak current, from 0.493 to 0.392, 0.364, 0.338, and 0.320 V respectively for curves B, C, D, E, and F in Figure 1.

It is important to note that, at higher ligand concentrations (curves C to F in Figure 1), the positive peak current resolves into two distinct peaks (labeled peak 1 and 2). The two peaks demonstrated the same trend: movement toward more negative potentials as the ligand concentration increases. The two peaks should be attributed to two different stoichiometries for the interfacial complexation reactions assisted by the TBP ligand.

Only a few groups reported discrete interfacial complexation reactions via the TIC mechanism. Dassie et al. and Kakiuchi and co-workers demonstrated two successive Cs^+ transfer waves (with metal-to-ligand ratios of 1:2 and 1:1) facilitated by dibenzo-18-crown-6 at w|DCE and w|RTIL interfaces, while Homolka and Wendt[31] reported transfer of multicomplexed Fe (II, III), Ni (II), and Zn (II) ions across the w|NB interface (ACT mechanism); yet, thermodynamic parameters were not well resolved. It was therefore worth evaluating these features individually. $\Delta_o^w\phi_{1/2}$ was approximated using the potential at the peak current ($\Delta_o^w\phi_p$) through eq 4.[53] Therefore, analysis of UO_2^{2+} FIT by TBP was carried out by means of the two half-wave potentials obtained. Due to the PPW end, only one sigmoidal wave was observed upon scanning the applied potential back, which represented the interfacial decomplexation reaction. This was also used for analysis.

As the ligand concentration was increased, the assisted ion transfer of metal species became more facile and the ML_n^{z+} peak moved to more negative potentials. It has been shown that a cation with hydrophilic character will demonstrate higher (or more positive) transfer potentials, while a hydrophilic anion will demonstrate the opposite, i.e., lower (or more negative) potentials.[42] While increasing the concentration of the ligand, it became easier

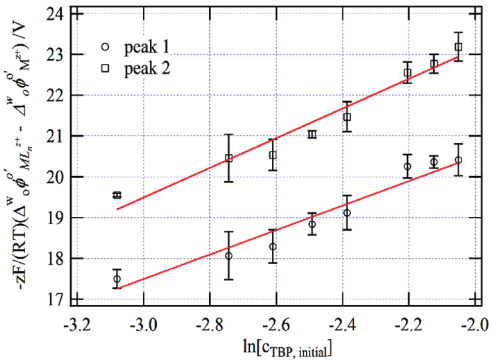

Figure 2. $\ln[c_{TBP,initial}]$ vs $-zF/(RT)(\Delta_o^w\phi_{ML_n^{z+}}^{o'} - \Delta_o^w\phi_{M^{z+}}^{o'})$ for the two curve features found in Figure 1: peak 1 (○) and peak 2 (□).

to transfer the metal species and the transfer potential for the cation decreased. By examination of this trend and using eq 5 developed by Girault et al.,[45] the metal to ligand stoichiometry (1:n) and the overall complexation constant (β) can be inferred:

$$-\frac{zF}{RT}(\Delta_o^w\phi_{ML_n^{z+}}^{o'} - \Delta_o^w\phi_{M^{z+}}^{o'}) = n\ln[c_{L,\,initial}] + \ln(\beta) \qquad (5)$$

where z is the charge of the metal−ligand complex and F, R, and T are the conventional thermodynamic parameters, specifically, Faraday's constant, the universal gas constant, and temperature in Kelvin, respectively. The initial concentration of the ligand in the organic phase at the beginning of the scan is defined by the term, $c_{L,initial}$.

Two considerations must be taken into account concerning electrochemically assisted complexation reactions at the micro-ITIES between w|DCE. First, the partitioning of free metal species into DCE (from $w \rightarrow o$) is considered to be negligible except where its transfer limits the PPW and, similarly, the ligand is considered miscible only in the organic phase. The mechanism of metal partitioning is therefore limited to transfer through interfacial complexation (TIC) of the metal with the ligand directly at the interface during the forward reaction and subsequently, during the reverse reaction, transfer through interfacial dissociation (TID). Two other extraction mechanisms have been identified[44,45] but are not considered: transfer of the metal species into the organic phase followed by organic phase complexation (TOC) and partitioning of the ligand species, $o \rightarrow w$, and then aqueous complexation followed by transfer (ACT).

Second, diffusion of species in the aqueous and DCE phases is considered equivalent ($D_{aq}^i = D_{org}^i$; where D_α^i is the diffusion coefficient of species i in phase α). Therefore, using eq 5 above, a linear relationship of $-zF/(RT)(\Delta_o^w\phi_{ML_n^{z+}}^{o'} - \Delta_o^w\phi_{M^{z+}}^{o'})$ vs $\ln[c_{TBP,initial}]$ was developed utilizing the data obtained from the series of CV experiments on Cell 1. In order to ensure accurate results, four CVs were taken at each ligand concentration; the full concentration range tested was from 18.3 to 137.9 mM. After careful analysis, it was decided to reject the first scan as it demonstrated inconsistent peak current results that were not comparable between ligand concentration steps; however, subsequent scans showed excellent agreement. A linear fit of these data was used to evaluate the metal to ligand ratio (1:n) and the complexation constant (β) through the slope and y-intercept of the line, respectively. Figure 2 illustrates the linear fitting data analysis of TBP assisted ion transfer of the uranyl ion based on the

dx.doi.org/10.1021/ac2018684 |Anal. Chem. 2011, 83, 7542–7549

Table 1. Results of the Linear Curve Fittings Shown in Figure 2 and Using eq 5[a]

ligand	curve feature	R^2	z_{eff}	n	β
TBP	peak 1	0.9728	1	3	3.2×10^{11}
	peals 2	0.9778	1	4	2.0×10^{13}

[a] Details the effective charge used (z_{eff}), stoichiometry (n), and complexation constant (β) for the two curve features: peaks 1 and 2.

two peak-shaped waves. The data garnered through this analysis are summarized in Table 1 which includes the R^2, z_{eff} (effective charge of the metal transferred), n, and β values.

The multiple stoichiometries analyzed using peaks 1 and 2 are shown in Figure 2 and demonstrate a very good linear relationship to the increasing ligand concentration; R^2 equal to 0.9728 and 0.9778, respectively. These data indicated a metal to ligand stoichiometry of approximately 1:3 and 1:4 while the complexation constants are 3.2×10^{11} and 3.9×10^{13} for peaks 1 and 2, respectively; both species were evaluated with an effective charge of 1+. Peak 2 is the most negatively shifted peak, indicating the ligand assisted metal transfer is more facile than that of peak 1, and this is consistent with the high ligand association and complexation constant observed. The more ligands coordinated to the metal center, the higher is the complexation constant, and, therefore, the more easily the metal will transfer.

The study by Homolka and Wendt[31] appeared in 1985, and their analysis was performed at a large-ITIES without the benefit of modern FIT theory.[44,45] In their report,[31] they assumed a static formal transfer potential for each metal to ligand stoichiometry and that increasing the ligand concentration leads to an increase in the peak current response. Presently, it has been shown that this is not the case and, using uranium as an example, when the ligand is in excess, the peak current is static and the potential shifts toward more positive potentials with increasing ligand concentration.[44,45,48] The analyses by Dassie et al.[59] and Kakiuchi et al.[48] were hampered by the fact that the two peaks they observed for the FIT of cesium with dibenzo-18-crown-6 were poorly resolved; however, computational curve fitting and simulation analysis overlaid on the experimental results allowed them to elucidate the stoichiometric ratios, complexation constants, and, thus, the mechanism of the reactions. What appears herein for the first time is the thermodynamic quantification of multiple, resolved FIT peaks at the micro-ITIES and using modern FIT theory.[44,45]

Moving forward, the data for two peaks were also evaluated using an effective charge of 2+ (data not shown), as is present in freely solvated uranyl ions, and leads to a ligand stoichiometry of 8. It may be possible for 8 TBP molecules to surround a single dioxouranuim cation. However, it was proposed that a single nitrate species participating in the complexation would reduce the net charge of the metal−ligand complex to 1+ and provide a sustainable metal/TBP ratio of 1:4. Qualitative examination of the NO_3^- IT peak reveals a slight drop in peak current intensity between the blank curve and the curves obtained after TBP was added. This drop in peak current is most likely indicative of a drop in the concentration of NO_3^- available for transfer and could be the result of two phenomena.

First, because the FIT portion of the CV was scanned first, the proposed uranyl−nitrato−TBP complex is initially transferred to the organic phase and then, on the reverse scan, transfers back to the aqueous phase. It follows that the system is most likely quasi-reversible and some complexed ions will be lost to the organic phase, thus reducing the nitrate concentration available for simple IT.

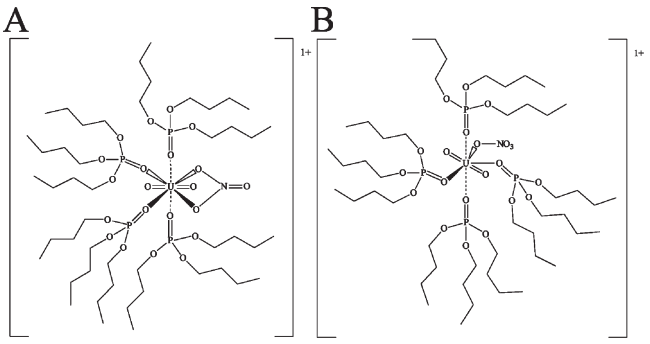

Figure 3. Proposed structures of (A) $UO_2NO_3TBP_4^+$ and (B) $UO_2NO_3TBP_3^+$.

Second, the structure of the liquid−liquid interface has been proposed to consist of a compact inner layer with bracketing diffuse layers[60−63] and has been evaluated using a model similar to the Gouy−Chapman theory for the metal−liquid interface. A measure of controversy remains concerning the, as yet to be described in detail, structure of the ITIES; however, all theories agree on the importance of adsorbed species at the interface as well as ion−ion interactions.[60−63] These adsorbed species would provide a mechanism whereby a completely hydrated uranyl ion may have its hydration sphere penetrated by a nitrate anion, thereby replacing one water molecule, and also reduce the amount of nitrate available for IT. Additionally, nitrate participation in the extraction process is in agreement with the neutral metal-nitrato species observed in the conventional PUREX/TRUEX processes[55,56] and is a fundamental requirement of these extraction procedures.

The maximum coordination number to the uranium (U) metal center (including the two oxygen species), of which we are currently aware, is 14,[64] and since uranium is such a large atom, the predominate force limiting this number is the steric hindrance between ligands. The formation of $UO_2NO_3TBP_n$ complexes with $n = 3$ and 4 provide a total coordination number of 7 and 8 with nitrate acting as a bidentate ligand; the proposed structures are shown in Figure 3A,B. The formation of UO_2 complexes with TBP of the form $UO_2(NO_3)_2(TBP)_2$ has long been identified,[55,56,65] and recently, UO_2 complexes with a high number of large organo-phosphorus complexing agents have also been demonstrated.[66,67] Powell et al.,[67] in their study of the radiolytic breakdown of TBP to dibutyl phosphoric acid (HDBP) in the storage tanks of UO_2 fuel recovered using the PUREX process, reported the formation of $UO_2(NO_3)_m(HDBP)_n$ with a NO_3^-/UO_2^{2+} ratio (m) of 0.9 and a $HDBP/UO_2^{2+}$ ratio (n) of 3.7, at high nitrate concentrations; this is evidence toward the viability of the UO_2-TBP proposed structures, as shown in Figure 3.

The proposed structures shown in Figure 3A,B illustrate hexagonal and pentagonal bipyramidal geometries for $n = 4$ and $n = 3$, respectively; please note, for simplicity, solvent molecules have been neglected.

Evaluation of Uranyl Facilitated Ion Transfer Using CMPO. Having quantified the FIT of the uranyl ion with TBP, attentions were turned to CMPO, the primary ligand of the TRUEX process. Figure 4 illustrates experimental progression of increasing CMPO concentration and its effect on the ML_n^{z+} peak using Cell 2.

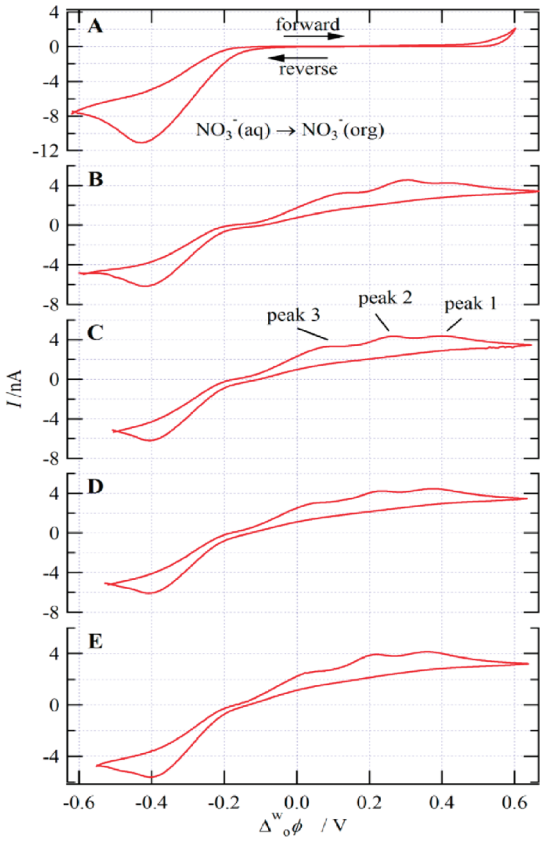

Figure 4. CMPO CV experiments utilizing Cell 2 with increasing CMPO concentration, 0.0, 9.5, 15.3, 22.7, and 31.1 for curves A, B, C, D, and E, respectively; the initial potential was set at −0.050 V, the upper and lower limits of the calibrated potential range were approximately 0.650 and −0.600 V, respectively, with a scan rate at 0.020 V·s−1.

The initial, calibrated potential was set equal to −0.050 V, and the upper and lower calibrated potential range was approximately 0.750 and −0.570 V. The blank CV, with no ligand added to the organic phase, is shown in Figure 4A that demonstrates no FIT during the forward scan, from 0.000 to 0.600 V, within the PPW. During the backward scan, the linear diffusion of nitrate in the aqueous phase and transfer into the organic phase was observed at −0.414 V as a peak shaped wave. After the lower switching potential is reached, the CV was swept again in the forward direction, from −0.570 to −0.050 V; the steady state current with a half-wave potential at −0.314 V was observed, and this is indicative of hemispherical diffusion of the nitrate species in the organic phase and transfer back across the interface from $o \rightarrow w$. After addition of CMPO, the FIT can be observed during the forward scan; however, three distinct current peaks can readily be distinguished. Just as in the case of TBP, the CMPO peak potentials were evaluated using eq 5. No singularly distinct steady state wave could be described and, therefore, could not be evaluated.

The metal:ligand stoichiometry and complexation constant evaluated for the three peaks were graphed in Figure 5A and B, indicating values of n equal to 2, 3, and 5 with β values of 8.0×10^{11}, 8.8×10^{14}, and 6.5×10^{32} for peaks 1, 2, and 3, respectively. These results are summarized in Table 2. As in the case of TBP, the effective charge of the metal transferred was considered to be 1+ with a nitrate molecule participating in the FIT for all cases

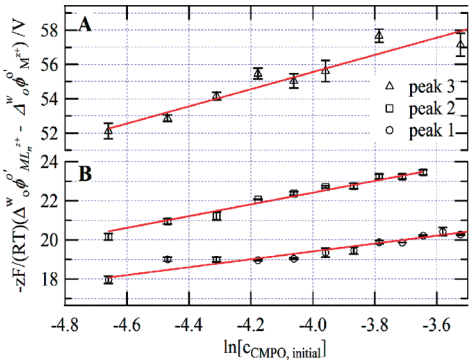

Figure 5. $\ln[c_{CMPO,initial}]$ vs $-zF/(RT)(\Delta^w_o\phi'_{ML_n^{z+}} - \Delta^w_o\phi'_{M^{z+}})$ for the three curve features found in Figure 4: (A) peak 3 (Δ); (B) peak 1(○) and peak 2 (□).

Table 2. Results of the Linear Curve Fittings Shown in Figure 5 and Using eq 5[a]

ligand	curve feature	R^2	z_{eff}	n	β
CMPO	peak 1	0.9593	1	2	8.0×10^{11}
	peak 2	0.9912	1	3	8.8×10^{14}
	peak 3	0.9586	2	5	6.2×10^{32}

[a] Details the effective charge used (z_{eff}), stoichiometry (n), and complexation constant (β) for the three curve features: peak 1, peak 2, and peak 3.

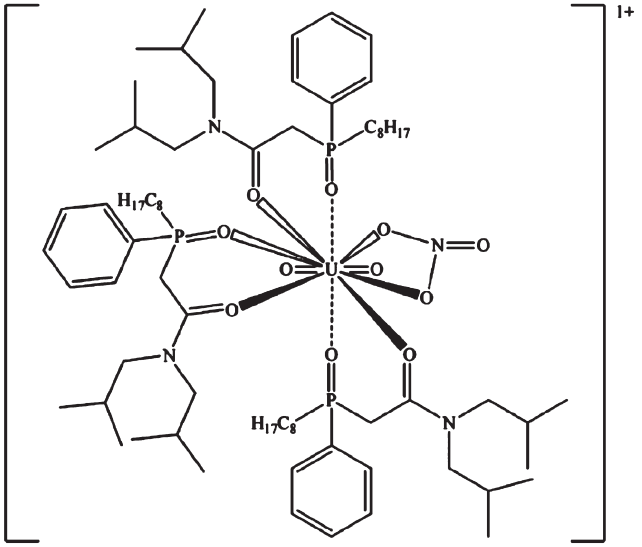

Figure 6. Proposed structure for one of the observed UO_2−CMPO complexes; $[UO_2NO_3CMPO_3]^+$.

except peak 3 which used the full 2+ charge. It is considered that a full charge of 2+ on the uranyl ion leads to a metal/ligand stoichiometry of 1:4 and 1:6 for peaks 1 and 2, respectively.

Interestingly, the size of the nitrate peak after addition of the ligand undergoes a dramatic change from 11.1 to 6.1 nA which indicates a large difference in the apparent nitrate concentration. This drastic change may indicate that CMPO FIT is trending from a quasi-reversible reaction to an irreversible one and also

dx.doi.org/10.1021/ac2018684 |Anal. Chem. 2011, 83, 7542–7549

lends further evidence to the proposed interaction of nitrate in the complexation reactions of both CMPO and TBP.

The β values and ligand stoichiometery agree well with the peak position order. The potential at peak 1 is more positive than peak 2, which demonstrates fewer ligands coordinated to the metal center at peak 1 than at peak 2. The stoichiometry is also consistent with the calculated β values; that is, β increases with each increase in the number of ligands participating in the complexation reaction: $\beta_{peak1,n=2} < \beta_{peak2,n=3} < \beta_{peak3,n=5}$.

The proposed structure of $[UO_2NO_3CMPO_3]^+$, shown in Figure 6, is consistent with the hexagonal bipyramidal geometry reported by Rogers et al. for bidentate CMPO in the $UO_2(NO_3)_2$-$CMPO_2$ complex.[13] The coordination number for $[UO_2NO_3$-$CMPO_n]^+$ is 8 and 10 for n equal to 2 and 3, respectively; CMPO is proposed to be bidentate. For n equal to 5 and 10 with all ligands considered monodentate, the total coordination numbers for these two complexes are 6 and 11. It has been shown that the most likely extraction route of lanthanides and trivalent actinides using CMPO is thought to occur (using Am^{3+} as an example) via:[9,19]

$$Am^{3+} + 3NO_3^- + 3CMPO \rightleftharpoons Am(NO_3)_3CMPO_3 \quad (6)$$

It is reasonable to conclude, therefore, that steric hindrance in the formation of $[UO_2NO_3CMPO_3]^+$ is not prohibitive and even $[UO_2CMPO_5]^{2+}$ and $[UO_2NO_3CMPO_{10}]^+$ are possible, although most likely are small contributors.

CONCLUSIONS

To the best of our knowledge, it is the first time to simultaneously evaluate distinct complexation steps using modern FIT theory[45,68] in an electrochemical micro-ITIES experiment. The complex stoichiometry of uranyl with TBP and CMPO, along with the quantitative evaluation of the complexation constant, β, garner a more holistic chemical description of FIT. Interfacial complexation reactions of uranyl with CMPO demonstrated three complexation constants equal to 8.0×10^{11}, 8.8×10^{14}, and 6.5×10^{32} for n equal to 2, 3, and 5, respectively, while those of uranyl with TBP showed β values of 3.2×10^{11} and 3.9×10^{13} for n equal to 3 and 4.

These results indicate that CMPO and TBP have similar complexation strengths since for $n = 2$ both show similar complexation constants. The electroanalytical chemistry at the micro interface presented here is simple, fast, and at low cost. It requires only a 300 μL sample containing the target metal ions for the analysis, which might open an avenue to analyze radioactive samples with minimum quantity. Our technique has the potential to evaluate these two and other ligands for lanthanide and actinide separations across a range of alternative solvents including room temperature ionic liquids.[13,14,24,25] This study may also open up the design of ion selective electrodes based on uranyl ligands.

AUTHOR INFORMATION

Corresponding Author

*Tel.: +1 519 661-2111 x 86161. Fax: +1 519 661-3022. E-mail: zfding@uwo.ca. URL: http://publish.uwo.ca/~zfding/.

ACKNOWLEDGMENT

We would like to thank J. Clara Wren, Jamie Noël, David W. Shoesmith, Paul J. Ragogna, John Vanstone, Jon Aukima, Justin Smith, Sherrie McPhee, and Marylou Hart for their helpful discussions and technical support. This work was supported by the Ontario Research Foundation, Natural Sciences and Engineering Research Council of Canada (NSERC), Canada Foundation for Innovation, Ontario Innovation Trust, the Premier's Research Excellence Award, and the University of Western Ontario. T.J.S. would like to thank the Department of Chemistry at the University of Western Ontario for "A Special International Research Experience" (ASPIRE) travel award and Prof. Hubert Girault at the Swiss Federal Institute of Technology in Lausanne for graciously accommodating a research exchange.

REFERENCES

(1) Zhang, W.; Ungar, K.; Hoffman, I.; Lawrie, R. *J. Radioanal. Nucl. Chem.* **2009**, *282*, 761–765.
(2) Leung, L. K. H.; Dimayuga, F. C. *Nucl. Eng. Des.* **2010**, *240*, 290–298.
(3) Lewis, B. J.; Iglesias, F. C.; Dickson, R. S.; Williams, A. *J. Nucl. Mater.* **2009**, *394*, 67–86.
(4) Marsh, G.; Davison, J. *Nucl. Eng. Des.* **2000**, *41*, 32–35.
(5) Nowierski, C.; Noel, J. J.; Shoesmith, D. W.; Ding, Z. *Electrochem. Commun.* **2009**, *11*, 1234–1236.
(6) Lumetta, G. J., Nash, K. L., Clark, S. B., Friese, J. I., Eds. *Separations for the Nuclear Fuel Cycle in the 21st Century*: American Chemical Society: Washington, DC, 2006.
(7) Paiva, A. P.; Malik, P. *J. Radioanal. Nucl. Chem.* **2004**, *261*, 485–496.
(8) Venkatesan, K. A.; Sukumaran, V.; Antony, M. P.; Srinivasan, T. G. *J. Nucl. Radiochem. Sci.* **2008**, *9*, 37–39.
(9) Fujii, T.; Yamana, H.; Watanabe, M.; Moriyama, H. *Solvent Extr. Ion Exch.* **2002**, *20*, 151–175.
(10) Giridhar, P.; Venkatesan, K. A.; Subramaniam, S.; Srinivasan, T. G.; Rao, P. R. V. *J. Alloys Compd.* **2008**, *448*, 104–108.
(11) Giridhar, P.; Venkatesan, K. A.; Srinivasan, T. G.; Rao, P. R. V. *J. Radioanal. Nucl. Chem.* **2005**, *265*, 31–38.
(12) Giridhar, P.; Venkatesan, K. A.; Srinivasan, T. G.; Rao, P. R. V. *J. Nucl. Radiochem. Sci.* **2004**, *5*, 21–26.
(13) Visser, A. E.; Jensen, M. P.; Laszak, I.; Nash, K. L.; Choppin, G. R.; Rogers, R. D. *Inorg. Chem.* **2003**, *42*, 2197–2199.
(14) Visser, A. E.; Rogers, R. D. *J. Solid State Chem.* **2003**, *171*, 109–113.
(15) Dietz, M. L.; Stepinski, D. C. *Talanta* **2008**, *75*, 598–603.
(16) Horwitz, E. P.; Schulz, W. W. In *Applied Science*; Elsevier: New York, 1991, p 21−29.
(17) Siddall, T. H., III *J. Inorg. Nucl. Chem.* **1963**, *25*, 883–892.
(18) Horwitz, E. P.; Dietz, M. L.; Nelson, D. M.; LaRosa, J. J.; Fairman, W. D. *Anal. Chim. Acta* **1990**, *238*, 263–271.
(19) Fujii, T.; Aoki, K.; Yamana, H. *Solvent Extr. Ion Exch.* **2006**, *24*, 347–357.
(20) Ansari, S. A.; Mohapatra, P. K.; Raut, D. R.; Kumar, M.; Rajeswari, B.; Manchanda, V. K. *J. Membr. Sci.* **2009**, *337*, 304–309.
(21) Vandegrift, G. F.; Chamberlain, D. B.; Conner, C.; Copple, J. M.; Dow, J. A.; Everson, L.; Hutter, J. C.; Leonard, R. A.; Nuñez, L.; Regalbuto, M. C.; Sedlet, J.; Srinivasan, B.; Weber, S.; Wygmans, D. G. In *Proceedings of the Symposium on Waste Management*; Post, R. G., Ed.; American Nuclear Society: Tuscon, Arizona, 1993; Vol. 2, p 1045−1050.
(22) Dai, S.; Ju, Y. H.; Barnes, C. E. *J. Chem. Soc., Dalton Trans.* **1999**, 1201–1202.
(23) Gaillard, C.; Moutiers, G.; Mariet, C.; Antoun, T.; Gadenne, B.; Hesemann, P.; Moreau, J. J. E.; Ouadi, A.; Labet, A.; Billard, I. *ACS Symp. Ser.* **2005**, *902*, 19–32.
(24) Nakashima, K.; Kubota, F.; Maruyama, T.; Goto, M. *Anal. Sci.* **2003**, *19*, 1097–1098.
(25) Chaumont, A.; Wipff, G. *Phys. Chem. Chem. Phys.* **2006**, *8*, 494–502.
(26) Luo, H.; Dai, S.; Bonnesen, P. V.; Buchanan, A. C. *J. Alloys Compd.* **2006**, *418*, 195–199.

(27) Luo, H.; Dai, S.; Bonnesen, P.; Haverlock, T.; Moyer, B.; Buchanan, A. *Solvent Extr. Ion Exch.* **2006**, *24*, 19–31.
(28) Murali, M. S.; Mathur, J. N. *Solvent Extr. Ion Exch.* **2001**, *19*, 61–77.
(29) Gatrone, R. C.; Rickert, P. G.; Horwitz, E. P.; Smith, B. F.; Bartholdi, C. S.; Martinez, A. M. *J. Chromatogr.* **1990**, *516*, 395–404.
(30) Wandlowski, T.; Marecek, V.; Samec, Z. *Electrochim. Acta* **1990**, *35*, 1173–1175.
(31) Homolka, D.; Wendt, H. *Ber. Bunsen-Ges. Phys. Chem.* **1985**, *89*, 1075–1082.
(32) Stockmann, T. J.; Ding, Z. *J. Electroanal. Chem.* **2010**, *649*, 23–31.
(33) Koryta, J. *Electrochim. Acta* **1979**, *24*, 293–300.
(34) Beattie, P. D.; Delay, A.; Girault, H. H. *Electrochim. Acta* **1995**, *40*, 2961–2969.
(35) Beattie, P. D.; Wellington, R. G.; Girault, H. H. *J. Electroanal. Chem.* **1995**, *396*, 317–323.
(36) Cacote, M. H. M.; Pereira, C. M.; Tomaszewski, L.; Girault, H. H.; Silva, F. *Electrochim. Acta* **2004**, *49*, 263–270.
(37) Taylor, G.; Girault, H. H. J. *J. Electroanal. Chem. Interfacial Electrochem.* **1986**, *208*, 179–183.
(38) Campbell, J. A.; Girault, H. H. *J. Electroanal. Chem. Interfacial Electrochem.* **1989**, *266*, 465–469.
(39) Wilke, S.; Zerihun, T. *Electrochim. Acta* **1998**, *44*, 15–22.
(40) Shao, Y. H.; Mirkin, M. V. *J. Phys. Chem. B* **1998**, *102*, 9915–9921.
(41) Langmaier, J.; Samec, Z. *Anal. Chem.* **2009**, *81*, 6382–6389.
(42) Samec, Z.; Langmaier, J.; Kakiuchi, T. *Pure Appl. Chem.* **2009**, *81*, 1473–1488.
(43) Langmaier, J.; Trojanek, A.; Samec, Z. *Electroanalysis* **2009**, *21*, 1977–1983.
(44) Reymond, F.; Carrupt, P.-A.; Girault, H. H. *J. Electroanal. Chem.* **1998**, *449*, 49–65.
(45) Reymond, F.; Lagger, G.; Carrupt, P.-A.; Girault, H. H. *J. Electroanal. Chem.* **1998**, *451*, 59–76.
(46) Shao, Y. H.; Mirkin, M. V. *Anal. Chem.* **1998**, *70*, 3155–3161.
(47) Josserand, J.; Morandini, J.; Lee, H. J.; Ferrigno, R.; Girault, H. H. *J. Electroanal. Chem.* **1999**, *468*, 42–52.
(48) Nishi, N.; Murakami, H.; Imakura, S.; Kakiuchi, T. *Anal. Chem.* **2006**, *78*, 5805–5812.
(49) Rodgers, P. J.; Amemiya, S. *Anal. Chem.* **2007**, *79*, 9276–9285.
(50) Gavach, C.; Henry, F. *J. Electroanal. Chem. Interfacial Electrochem.* **1974**, *54*, 361–370.
(51) Parker, A. J. *Electrochim. Acta* **1976**, *21*, 671–679.
(52) Shao, Y.; Stewart, A. A.; Girault, H. H. *J. Chem. Soc., Faraday Trans.* **1991**, *87*, 2593–2597.
(53) Bard, A. J.; Faulkner, L. R. *Electrochemical Methods: Fundamentals and Applications*, 2nd ed.; John Wiley: New York, 2001.
(54) Stockmann, T. J.; Olaya, A. J.; Méndez, M. A.; Girault, H. H.; Ding, Z. *Electroanalysis* **2011**, DOI: 10.1002/elan.201100401.
(55) Burns, J. H. *Inorg. Chem.* **1983**, *22*, 1174–1178.
(56) Burns, J. H. *Inorg. Chem.* **1981**, *20*, 3868–3871.
(57) Akhila Maheswari, M.; Subramanian, M. S. *Talanta* **2004**, *64*, 202–209.
(58) Birkett, J. E.; Carrott, M. J.; Fox, O. D.; Jones, C. J.; Maher, C. J.; Roube, C. V.; Taylor, R. J.; Woodhead, D. A. *J. Nucl. Sci. Technol.* **2007**, *44*, 337–343.
(59) Dassie, S. A.; Yudi, L. M.; Baruzzi, A. M. *J. Electroanal. Chem.* **1999**, *464*, 54–60.
(60) Gavach, C.; Seta, P.; D'Epenoux, B. *J. Electroanal. Chem.* **1977**, *83*, 225–235.
(61) Daikhin, L. I.; Kornyshev, A. A.; Urbakh, M. *J. Electroanal. Chem.* **2001**, *500*, 461–470.
(62) Daikhin, L. I.; Urbakh, M. *J. Electroanal. Chem.* **2003**, *560*, 59–67.
(63) Su, B.; Eugster, N.; Girault, H. H. *J. Electroanal. Chem.* **2005**, *577*, 187–196.
(64) Bernstein, E. R.; Hamilton, W. C.; Keiderling, T. A.; La Placa, S. J.; Lippard, S. J.; Mayerle, J. J. *Inorg. Chem.* **1972**, *11*, 3009–3016.
(65) Shukla, J. P.; Misra, S. K. *J. Membr. Sci.* **1991**, *64*, 93–102.
(66) Bagnall, K. W.; Wakerley, M. W. *J. Inorg. Nucl. Chem.* **1975**, *37*, 329–330.
(67) Powell, B. A.; Navratil, J. D.; Thompson, M. C. *Solvent Extr. Ion Exch.* **2003**, *21*, 347–368.
(68) Homolka, D.; Holub, K.; Marecek, V. *J. Electroanal. Chem. Interfacial Electrochem.* **1982**, *138*, 29–36.